CrossMark
click for updates

Growth behavior of water dispersed MgAl layered double hydroxide nanosheets†

Xiujiang Pang,*[a] Li Chen,[b] Yuan Liu,[c] Mingjun Chi,[b] Zaifeng Li*[a] and Johann Plank[d]

Water-dispersed LDH nanosheets prepared using a microreactor could be used as building blocks for LDH-based functional materials. Elucidating the growth behavior of LDH nanosheets in aqueous phase helps to obtain its aqueous dispersion for further application in different fields. In this paper, a two stage growth behavior of LDH nanosheets was proposed which was based on the results of transmittance, viscosity, pH value, size distribution and morphological features of crystallites. In the first stage, MgAl-LDH nanosheet gel was dispersive in aqueous phase and the lateral size of nanosheets grew progressively, while in the second stage, the nanosheets stacked to build a three-dimensional network and the integrated plate-like structure of LDH was formed progressively. For both stages, curves of pH *versus* standing time implied the growth behavior fitted a first-order model. The results of both transmittance and viscosity indicated that the dispersion degree and nanosheet stacking rate were temperature dependent and independent of concentration. A diagram including three regions was made, which could be used to determine the state of the LDH nanosheets in aqueous phase and could also provide a theoretical basis for the practical application of LDH nanosheets.

Introduction

Layered double hydroxides (LDHs), are an extensive class of ionic lamellar compounds made up of positively charged brucite-like layers with an interlayer region containing charge compensating anions and solvation molecules. The general formula of LDHs may be described as $[M_{1-X}^{2+}M_X^{3+}(OH)_2]^{X+}(A_{x/n}^{n-})\cdot mH_2O$, where M^{2+} and M^{3+} are divalent and trivalent metal cations which occupy octahedral holes in a brucite-like layer, and A^{n-} can be various kinds of inorganic or organic anion which are located in the hydrated interlayer galleries.[1] The chemistry of LDHs is now widely studied driven by the use of these materials as precursors for preparing CO_2 adsorbents,[2] catalysts,[3,4] fire retardant additives,[5] polymer/LDH nanocomposites,[6,7] drug delivery hosts,[8] electrochemical storage materials[9] and cement additives.[10]

So far the preparation of LDH mainly includes particles and nanosheets. For LDH particles, in general, the most commonly used method is coprecipitation at varied or constant pH, followed by aging at a certain temperature.[11,12] But as is well known, it is difficult for traditional methods to offer uniform precipitation conditions. Firstly, there is a gradient of supersaturation due to the limitation of mixing and heat transfer in batch reactor, which affects the nucleation and growth stages dramatically. Secondly, because of intermittent operation mode, the residence time of precipitate particles varies from the beginning to the end of precipitation behavior, which inevitably leads to a wide particle size distribution and poor reproducibility. Furthermore, considering the scale-up effect of batch reactor, the result in a lab is difficult to be replicated on a mass production.[13,14] To solve these problems, microreactor is often used to prepare nanoparticles for the reactant can be well mixed in a limited space, and the nucleation and ageing behavior can be separated immediately.[14–17]

Different from the traditional LDH particles prepared by coprecipitation method, the anisotropy of LDH nanosheets allows their use as ideal 2D quantum systems for studying fundamental physics, or as building blocks for functional materials.[18–23] The delamination of LDHs has been widely reported.[18–20] The synthesis of LDH nanosheets was first reported by Hu *et al.* *via* a reverse (water-in-oil) microemulsion method.[24] Water droplets acted as microreactors, in which LDH nanosheets were formed because of limited space and reactant availability. Liang *et al.* obtained MgAl-LDH nanosheets in formamide by a co-precipitation method.[25] All of the above

[a]State Key Laboratory Base of Eco-chemical Engineering, College of Chemistry and Molecular Engineering, Qingdao University of Science and Technology, Qingdao 266042, P. R. China. E-mail: xiujiangpang@qust.edu.cn; lizfengphd@126.com

[b]Key Laboratory of Rubber & Plastics, Ministry of Education/Shandong Provincial Key Laboratory of Rubber and Plastics, Qingdao University of Science and Technology, Qingdao 266042, P. R. China

[c]College of Petroleum Engineering, China University of Petroleum (East China), Qingdao 266042, P. R. China

[d]Technische Universität München, Chair for Construction Chemicals, Garching 85747, Germany

† Electronic supplementary information (ESI) available: XRD patterns of MgAl-LDH nanosheets standing for different times. See DOI: 10.1039/c7ra00833c

methods to prepare LDH nanosheets had problems of the using of toxic solvents, the adsorption of organic substances on the obtained nanosheets, or the difficulty in large-scale preparation, which all limited the actual application of LDH nanosheets. Our group successfully obtained LDH with narrow distribution by continuous precipitation using a T-type microchannel reactor. More interestingly, the obtained LDH was consisted of 1–2 brucite-like layers.[26] This method is simple, environmentally friendly and can realize the large-scale preparation. Moreover, we also explored its further application in fabricating LDH-based materials, such as drug delivery[27,28] and hydrophobic protective coatings,[29] which exhibited its advantage of controllable surface modification.

For controllable preparation and further application, the deep insight of LDH formation mechanism was needed, and various schemes have been proposed based on different syntheses.[30–33] Synthesizing LDHs by coprecipitation usually includes two stages: initial coprecipitation and subsequent peptizing (or aging). Braterman *et al.*[30,31] suggested that poorly crystallized LDH was formed during coprecipitation, which was then converted to well-crystallized LDH during aging. Eliseev *et al.*[32] noted that agglomerates formed during coprecipitation were amorphous, but then converted into a layered structure during aging. Chang *et al.*[33] obtained size-sorted LDH nanosheets by their lateral sizes using a density gradient ultracentrifuge separation technique, and proposed a four-stage formation behavior, *i.e.*, firstly, the coprecipitation of amorphous aluminum hydroxide and magnesium hydroxide, and then the absorbed magnesium salts redissolved into the solutions, thirdly, the formation of the LDH crystal nucleus with different Mg/Al ratios by aluminum atoms diffusing into magnesium hydroxide structures and finally growth/crystallization of the LDH crystal nucleus occurred *via* a hydrothermal treatment. Apparently, all these different models have been based on their different observations under different experimental conditions, reflecting the complexity of the LDH formation behavior.

Different from traditional coprecipitation, LDH nanosheets crystal formed by one-step in a short time after salts and alki solution being mixed in the junction of a T-type microreactor. The naked LDH nanosheets prepared in aqueous phase has good application prospects in many fields. The stability is very important for the further application, so we designed a series of experiments to explore the growth behavior.

In this work, we report a systematic investigation of the growth behavior of MgAl-LDH nanosheets dispersed in aqueous phase by studying the dependence of transmittance, viscosity, pH value and the morphology of the LDH upon time. LDH's growth behavior was discussed based on the characterization results. Then, a temperature–time diagram and a possible growth behavior were proposed, and by which the dispersion state of LDH nanosheets in aqueous phase could be determined. We hope our detailed understanding of the growth behavior of LDH nanosheets in aqueous phase will be of considerable importance for preparing LDH-based materials.

Experimental section

Materials

All chemicals were of analytical grade and were used as received from BASF Co., Ltd. (China). Ultrapure water with resistivity of 18.2 MΩ cm from an AFZ-1000-U purification system (China) was used throughout this study.

Preparation of MgAl LDH nanosheets

MgAl–NO$_3$ LDH was synthesized by coprecipitation using a T-type microreactor.[26] The concentration of mixed salt solution (Mg^{2+} + Al^{3+}) was 0.3 mol L^{-1} and Mg/Al molar ratio was 2 by dissolving 0.750 g (2 × 10^{-3} mol) Al(NO$_3$)$_3$·9H$_2$O and 1.026 g (4 × 10^{-3} mol) Mg(NO$_3$)$_2$·6H$_2$O in 20 mL water. The alkali solution was diluted NH$_3$·H$_2$O solution (∼7 wt%). These two solutions were pumped into the microreactor through two inlets, each at a flow rate of 20 mL min^{-1}. The resulting suspension was collected at the reactor outlet, and centrifuged at 12 000 rpm to remove the supernatant. The precipitate was washed three times with water by redispersion/centrifugation, yielding LDH nanosheets as a gel. The synthesis was carried out at ambient temperature (∼25 °C). Transmittance, viscosity, morphology, pH value and size distribution were discussed on LDH dispersion in aqueous phase with different solid content and standing time.

Characterization techniques

A Seiko SPA 400 model atomic force microscopy (AFM) system was used to examine the surface topography of nanosheets deposited on mica wafers. AFM images were acquired in tapping mode, using a Si tip cantilever with a force constant of 20 N m^{-1}. The transmittance of LDH dispersions was measured on a UV-1901 UV-vis spectrophotometer at λ = 590 nm. Particle size distributions were determined using a Malvern Mastersizer 2000 laser particle size analyzer. The viscosity of LDH dispersions was measured by a C-LTD80/QC rheometer, at a shear rate and temperature of 200 s^{-1} and 25.0 ± 0.5 °C, respectively. The pH value was measured by a S220-K pH meter at atmosphere temperature.

Results and discussion

The stability of the LDH nanosheets was first investigated by observing the macroscopic aspect. Then the influence of time and temperature on pH value of the aqueous dispersion, the change of the lateral size, thickness and particle size distribution, the transmittance and viscosity were investigated. Finally, a growth behavior was supposed according to the above experiment results.

Macroscopic aspect

The gel-like MgAl-LDH (solid content of 7.0 wt%) was put into transparent glass bottle and the change of its macroscopic properties could be easily observed (Fig. 1). After standing for 2 days, the white gel progressively transformed into translucent sol, and the fluidity increased with time. The possible reason is that the product aggregated after centrifugation and existed as

cluster after being dispersed into aqueous for a short time, and then they dispersed progressively as nanosheets due to electrostatic repulsion between positive charged LDH nanosheets. The gel became slightly turbid after 7 days. After peptized at 60 °C for 48 h, it turned into white suspension for the growth of nanosheet along ab-plate and the stacking along c-axis (which is perpendicular to ab-plate) as reported.[26] Moreover, it is worth to note there wasn't precipitation observed, which indicate the obtained LDH had a high aqueous colloidal stability.

pH value measurement

MgAl-LDH was prepared using a microreactor and centrifuged at 12 000 rpm to remove the supernatant. One part of sample without washing was dispersed in aqueous phase, and stood at 25 °C. The rest was divided into three parts and washed twice with deioned water and dispersed in aqueous phase, and then let stand at the temperature of 25 °C, 35 °C and 40 °C, respectively. The solid concentration of all samples is 29.8 g L^{-1}. For exploring the crystal growth of LDH nanosheets, pH value was measured at intervals. Fig. 2 showed curves of pH value *versus* time. pH decreased from 10.0 to 9.7 in 35 hours for unwashed sample, and decreased from 9.55 to 9.25 for washed sample, indicating the consumption rate of OH$^-$ was slow. It was worth noting that the curve of unwashed sample was almost parallel to that of washed sample at the same standing temperature, and both curves had an inflection point at a standing time of 35 hours. For samples standing at 35 °C and 40 °C, curves were divided into two parts, and for each part there was a good linear relationship between pH and time. The pH value in the first part decreased less than that in the second part. The first stage became shorter with the increase of temperature, and the inflection points appeared at the standing time of 17 h and 12 h under the temperature of 35 °C and 40 °C, respectively.

According to the above results, the crystal growth behavior can be regarded as the further reaction of cations with ions on fresh LDH nanosheets, so it could be represented by formula as

$$LDH_1 \cdot [M^{2+} + M^{3+} + OH^-] \rightarrow LDH_2 \quad (1)$$

where LDH$_1$ was the fresh LDH nanosheets, LDH$_2$ the LDH at the standing time of t, M^{2+} the Mg^{2+}, M^{3+} the Al^{3+}, '·' represented cations and anions adsorbed on the surface of LDH$_1$ and reacted on it. So the rate equation can be represented as

$$-\frac{dc_{OH^-}}{dt} = k[M^{2+}]^\alpha [M^{3+}]^\beta [OH^-]^\gamma \quad (2)$$

where k is the reaction rate constant, α, β, γ is the reaction order.

Fig. 1 Macroscopic aspect of gel-like MgAl-LDH (solid content of 7.0 wt%) prepared using a microreactor standing for different time at 25 °C and peptized at 60 °C for 48 h.
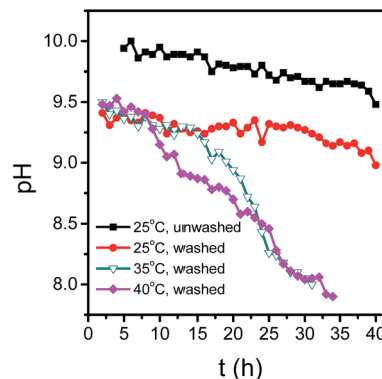

Fig. 2 The change of pH value during the growth process of LDH nanosheets.

As we all know lg c_{OH^-} = pH − 14, so lg c_{OH^-} is in reverse proportion to the standing time according to the results of Fig. 2, conforming to the characteristic of first order kinetic equation. So, $\alpha = 0$, $\beta = 0$, $\gamma = 1$.

Furthermore, eqn (2) can be rewritten as follows,

$$-\frac{dc_{OH^-}}{dt} = kc_{OH^-} \quad (3)$$

$$-2.303 d\lg c_{OH^-} = kdt \quad (4)$$

$$-2.303 d(pH - 14) = kdt \quad (5)$$

$$\frac{dpH}{dt} = -\frac{k}{2.303} \quad (6)$$

According to the slope for plot of pH–t, the reaction rate constant for the first stage can be calculated as 0.022, 0.049, and 0.082 for 25 °C, 35 °C and 40 °C, respectively.

AFM measurement

Fig. 3 shows a tapping-mode AFM image of LDH particles collected from the sample standing for 15 h, 23 h and 32 h, respectively. For samples of 15 h and 23 h, LDH nanosheets had a thickness and lateral size of 0.6–0.9 and 20–40 nm, respectively (Fig. 3A, A1 and B, B1), which had the same size with the fresh LDH.[26] The thickness of a brucite-like layer is *ca.* 0.48 nm,[34] and the d-spacing of the LDH sample was 0.87 nm.[26] Thus, LDH nanosheets were estimated to consist of 1–2 brucite-like layers.[35,36] After standing for 32 h, LDH nanosheets had lateral size and a thickness of 30–50 and 1.5–3.0 nm, respectively (Fig. 3C, C1), indicating that the nanosheets grew along ab-plate and packed to 2–4 layers along c-axis which is perpendicular to ab-plate. According to the above results, the nanosheets grew slowly along ab-plate before the standing time of 32 h.

DLS measurement

Particle size distributions were measured to determine the evolution process of size distribution (Fig. 4). The particle size was 25–45 nm for 15 h and 23 h, and became 25–60 nm for 32 h. And then, the LDH crystal grew more quickly and the particle
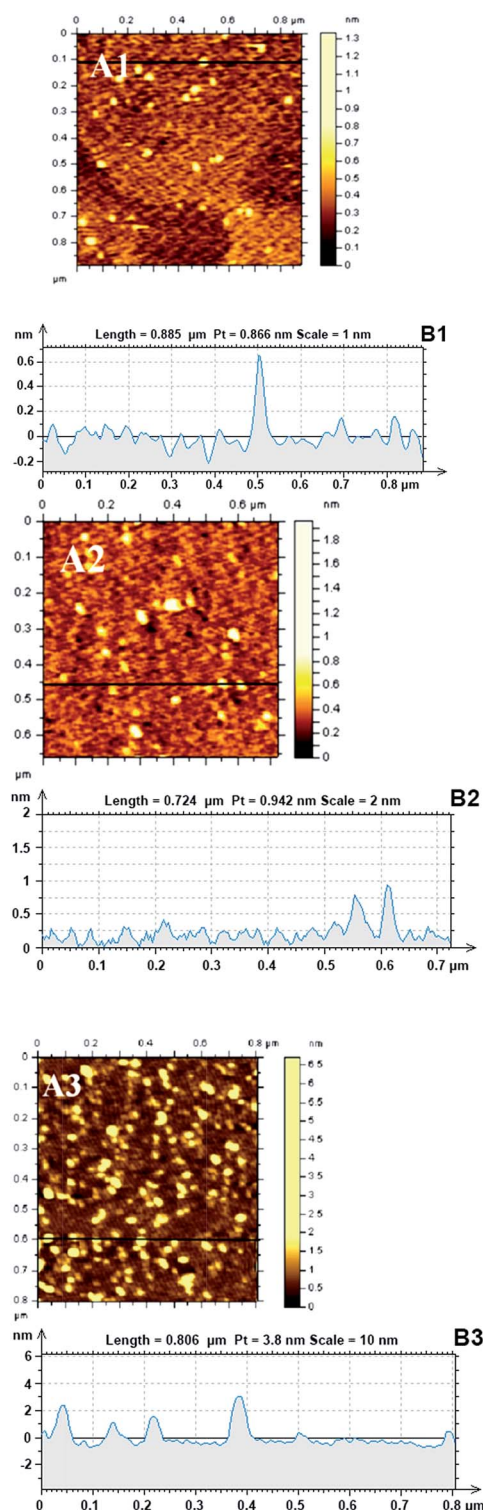
Fig. 3 (A) AFM image and height scale of LDH nanosheets collected from sample standing for different times, and (B) sectional analysis along the black line marked in (A). (A1, B1) 15 h, (A2, B2) 23 h, and (A3, B3) 32 h.

size distribution was 35–90 nm for 40 h. For peptized LDH, it was about 70–120 nm. The evolution observed from the results of DLS showed that the particles grew larger with time though they grew slowly before 32 h.
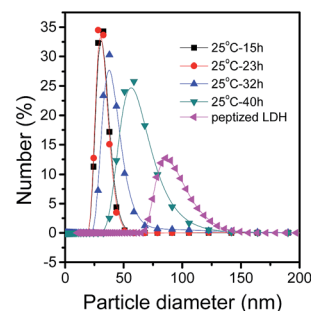

Fig. 4 Particle size distributions of LDH particles collected from sample standing for different times at 25 °C.

Transmittance measurement

Fig. 5 showed curves of transmittance (T) *versus* standing time (t) of LDH dispersion with different solid concentration at 25 °C. It was interesting that transmittance reached a maximum at the standing time about 32 h regardless of solid concentration. The dispersion behavior can be represented as $(LDH)_n \rightarrow nLDH$. Providing the initial solid content of $(LDH)_n$ and LDH nanosheets is C_s and zero, respectively, and the solid concentration of LDH nanosheets is C_N after $(LDH)_n$ were dispersed in aqueous phase for a standing time of t. The dispersion process was supposed to be uniform, then the solid concentration of LDH nanosheets (C_N) can be represented as $C_N = f_T C_s$, in which f_T is the dispersion fraction (a definition for dispersion degree) and is a constant at a certain temperature regardless of solid concentration. For MgAl-LDH nanosheets, f_T is about $t/32$ at 25 °C. For sample with solid concentration of 29.8 g L^{-1}, the transmittance was lower than 1% before the standing time of 11 hours, although 11/32 of LDH nanosheets were dispersed, the transmittance was still quite low due to a high solid concentration. So we can estimate the first stage will appear obviously if the solid concentration is more than 19.6 g L^{-1} at 25 °C.

For further exploring whether the maximum transmittance keep unchanged or not for samples with different solid concentration at the same temperature, the effect of the solid concentration on transmittance with time was investigated. Fig. 6 showed that the maxima of the transmittance appeared at the time of 32 h for samples with different solid concentration. Moreover, it was obvious that the change trend is quite different
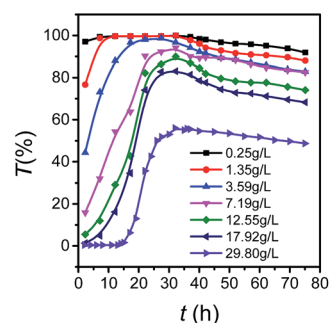

Fig. 5 The relationship between transmittance and time of samples with different solid concentration at the temperature of 25 °C.
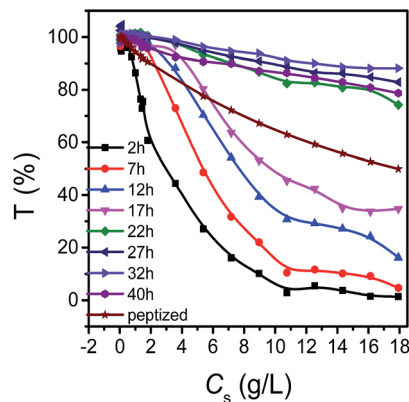
Paper

Fig. 6 The effect of the solid concentration on transmittance at different growth time under the temperature of 25 °C.

for different standing time. For samples standing for 2–17 h, the transmittance declined fast firstly and then gradually became steady with the increase of the solid concentration, but for samples standing for 22–40 h, it declined slowly. While for peptized LDH, the transmittance decreased almost linearly with solid concentration increasing.

Curves of $\lg T$ *versus* t were plotted (Fig. 7A) for better observing the growth behavior. For the sample with a solid concentration of 29.8 g L^{-1}, the $\lg T$–t curve was divided into three parts. The first part was a straight line and the transmittance was close to zero because LDH nanosheets aggregated into clusters. No first stage was observed for the samples with solid concentration of 0.25–17.92 g L^{-1} because LDH nanosheets dispersed better at lower solid concentration. For the second part, a quite good linearity appeared between $\lg T$ and t, and the slope decreased with the decrease of solid concentration. According to the AFM results, during this process nanosheets grew along ab-plate and there was no packing of nanosheets along c-axis, which had little influence on transmittance. So the transmittance change was mainly caused by the variation in the dispersion degree of nanosheets in aqueous phase. It is worthy to mention there were nonlinear regions (denoted by circle) near the turning point between the second part and the third part which is probably due to the transmittance was influenced by a combination of several coexisting factors such as dispersion degree, growth along ab-plate and c-axis. For the third part, there was a decrease in transmittance. According to the results of XRD (Fig. 1S, ESI†), in this part, LDH nanosheets stacked along c-axis, and then a three-dimensional network and the integrated plate-like structure of LDH was formed progressively. Meanwhile, the LDH also grew along ab-plate as reported.[26]

Moreover, it was interesting that the slope was the same for samples with different solid concentration, suggesting that the stacking rate was independent of solid concentration. According to the above results, for the second and the third parts, the relationship between $\lg T$ and t can be represented with the following formula as $\left(\frac{\partial \lg T}{\partial t}\right)_{C_s} = k_a$, where k_a is the slope of $\lg T$–
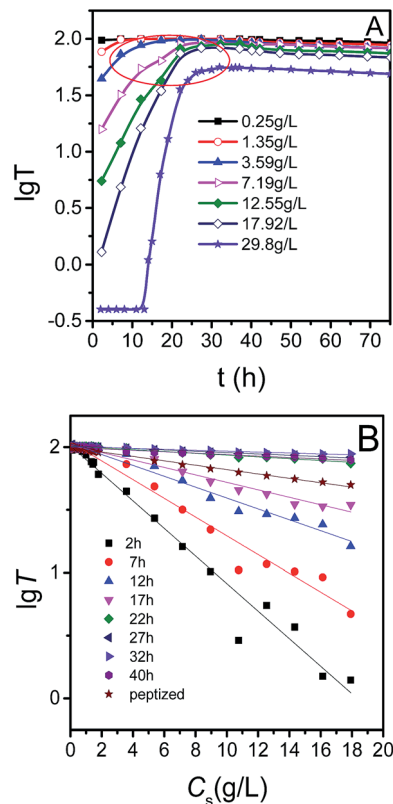

Fig. 7 The relationship of (A) $\lg T$ and t, (B) $\lg T$ and C_s.

t plot. For the samples with solid concentration varying in the experimental range (0–18 g L^{-1}), $\lg T$ changed linearly with C_s increasing (Fig. 6B), which can be described with a equation as $\left(\frac{\partial \lg T}{\partial C_s}\right)_t = k_b$, where k_b is the slope of $\lg T$–C_s plot.

Above all, results of Fig. 7A and B showed that $\lg T$ is a function of t and C_s at the same temperature, and it can be described as the following eqn (7) and (8):

$$\mathrm{d}\lg T = \left(\frac{\partial \lg T}{\partial t}\right)_{C_s} \mathrm{d}t + \left(\frac{\partial \lg T}{\partial C_s}\right)_t \mathrm{d}C_s, \tag{7}$$

and

$$\mathrm{d}\lg T = k_a \mathrm{d}t + k_b \mathrm{d}C_s \tag{8}$$

where k_a increased with C_s for the second part, while almost a constant for samples with different solid content for the third part.

In order to study the effect of temperature on growth behavior of LDH nanosheets in aqueous phase, the relationship between transmittance (T) and standing time (t) for LDH aqueous dispersion with a solid content (C_s) of 29.8 g L^{-1} at different temperature (Fig. 8) was presented. All curves appeared S-type and could be divided into three parts. For the initial horizontal part, the transmittances were close to zero, and the higher the temperature, the shorter the time of the first part. For the second part, transmittance rose and the slope elevated with the increase of temperature, which suggests that
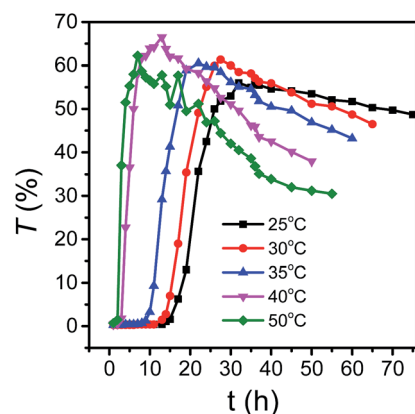
Fig. 8 Curves of transmittance *versus* time at different temperature with solid concentration of 29.8 g L^{-1}.

the dispersion rate improved with the temperature. For the third part, the transmittance decreased, and the higher the temperature, the faster the transmittance decreased, indicating the nanosheets' stacking rate increased with temperature. After being treated for more than 50 h at 50 °C, the transmittance changed little, implying the crystal growth was completed. So it could be concluded that dispersion degree and stacking rate of LDH nanosheets were determined by temperature.

Viscosity measurements

Fig. 9A showed the plots of viscosity as a function of shear rate for sample standing at 35 °C for different time lengths. By
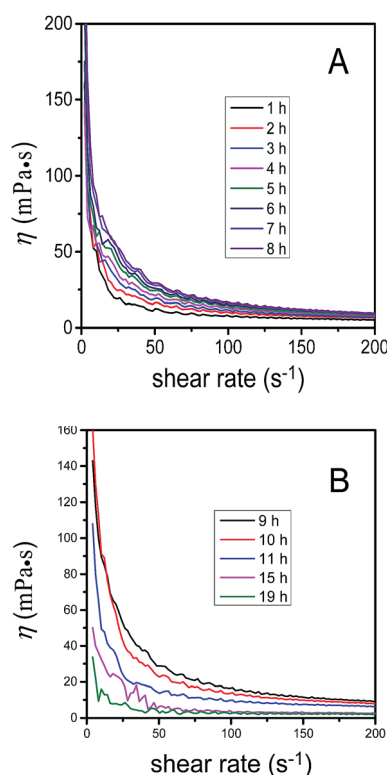

Fig. 9 Plot of viscosity as a function of shear rate for sample at 35 °C for different standing time. (A) From 1–8 h, (B) 9–19 h.

analysing the relationship between viscosity and shear rate, the dispersions of LDH nanosheets showed shear thinning phenomena with shear rate increasing. The observed viscosity behavior could be explained by the classical house-of-cards structure that consists of sheets arranged in a random edge-to-face orientation that leads to the formation of a gel.[37,38] The randomly arranged microstructure would lead to a dispersion with high viscosity. The LDH sheets would align themselves parallel to each other upon applying shear force, thereby the friction and hence the viscosity both decreased. Moreover, it was obvious that the viscosity increased upon standing from 1 to 8 h, and the reason is not clear yet and need further exploration. Fig. 9B showed curves between viscosity and shear rate when the standing time varied from 9 to 19 h. The viscosity decreased obviously with time lengthening, which probably because more and more nanosheets dispersed in aqueous phase. It was worthy noting that the viscosity decreased rapidly to about 2 mPa s while the standing time exceeded 15 h. Another structure wherein the LDH sheets stack in a parallel platelike arrangement could explain the viscosity behavior. The application of a small shear would be sufficient for the already parallel platelets to slide over each other and show shear-induced thinning.[37,39]

To better understand the growth behavior of LDH nanosheets, viscosity of the LDH dispersion with C_s 29.8 g L^{-1} *versus* standing time (t) at different time were examined at a shear rate of 200 s^{-1}, as shown in Fig. 10. All curves of η–t were reverse S-shape and could be divided into three parts. Viscosity increased at the first stage, and almost remained unchanged at the third stage. Moreover, similar with the results of the transmittance, the standing time of the first stage became shorter and the slope of the second stage increased with the temperature, which could be attributed to the rapid dispersion of LDH nanosheets at high temperature. Compared with Fig. 5, the transmittance change could not be detected at high solid concentration at the first stage, and for the third stage, the viscosity was nearly invariable with time while the transmittance decreased obviously due to the stacking of the nanosheets. So the viscosity and the transmittance measurement complement each other well in disclosing the growth behavior of water dispersed LDH nanosheets.
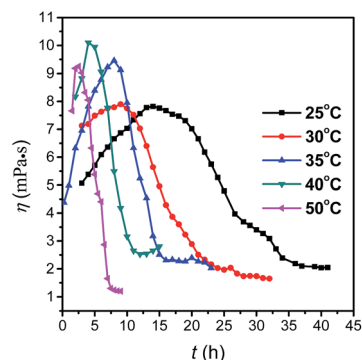

Fig. 10 Viscosity of MgAl-LDH dispersion (29.8 g L^{-1}) *versus* standing time at different temperature, at a shear rate of 200 s^{-1}.

Table 1 Inflection points of curves of $T-t$ and $\eta-t$

$T/°C$	The first inflection point		The second inflection point	
	$\eta-t$	$T-t$	$\eta-t$	$T-t$
25	14	15	32	32
30	12	12	20	21
35	9	8	16	16
40	4	3	12	12
50	2.5	2	7	7

The dispersion state of nanosheets and growth schematic model

The inflection points of curves obtained from Fig. 5 and 10 were listed in Table 1, and the inflection points of viscosity curves were quite consistent with that of transmittance.

According to Table 1, for MgAl-LDH with solid concentration of 29.8 g L^{-1}, a graph of time–temperature can be divided into three regions by the lines of a and b in Fig. 11. The growth behavior of MgAl-LDH nanosheets in aqueous phase was also summarized in Scheme 1. There were mainly two steps, *i.e.*, dispersion and stacking of nanosheets. In region I and region II, nanosheets dispersed progressively in aqueous phase and grew slightly along the ab-plate without stacking along *c*-axis. In region I, the LDH nanosheets mainly existed in cluster, and in region II the nanosheets dispersed obviously, and the closer to line b, the higher the dispersion degree. In region III, the nanosheets stacked in a parallel platelike arrangement and grew along ab-plate in the meanwhile, and the farther away from line b, the larger the size of LDH particles. The diagram might function as a phase diagram. For example, fresh MgAl-LDH nanosheets dispersed in aqueous with a solid concentration of 29.8 g L^{-1} was set at 32.5 °C (point *P*) and the nanosheets state would change along line PM upon standing for several hours. After 17.5 hours, the point moved from *P* to *M* which was closed to line b, and MgAl-LDH were dispersed as nanosheets in aqueous. So, such a diagram with division of different regions
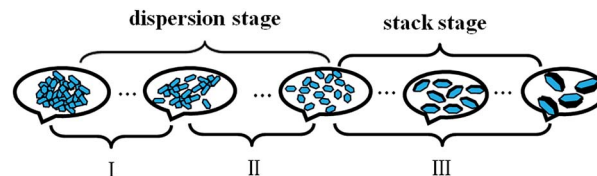
Scheme 1 Schematic diagram of MgAl-LDH nanosheets with solid concentration of 29.8 g L^{-1} in water dispersion and the dispersing state of LDH upon standing.

could provide valuable theoretical foundation for the controllable fabrication of LDH nanosheets and their practical application.

Conclusions

To clearly reveal the growth behavior of LDH nanosheets in aqueous phase, the direct information was obtained according to the whole experimental results, and a two stage growth behavior was proposed. In the first stage, the dispersion was a main behavior and the nanosheets grew slightly along the lateral direction. While in the second stage, the nanosheets stacked progressively, accompanied with the lateral growth. The LDH nanosheets' growth behavior can be expressed in a first-order model according to the results of pH variation during growth process. A time–temperature diagram was made based on the inflection points for the curves of $T–t$ and $\eta–t$, by which the dispersion state of LDH nanosheets was determined, which would be quite useful for directing the application of the LDH nanosheets in different fields.

Acknowledgements

References

1 F. Cavani, F. Trifiro and A. Vaccari, Hydrotalcite-type anionic clays: Preparation, properties and applications, *Catal. Today*, 1991, **11**, 173–302.

2 Q. Wang, H. H. Tay, Z. Guo, L. Chen, Y. Liu, J. Chang, Z. Zhong, J. Luo and A. Borgna, Morphology and composition controllable synthesis of Mg–Al–CO$_3$ hydrotalcites by tuning the synthesis pH and the CO$_2$ capture capacity, *Appl. Clay Sci.*, 2012, **55**, 18–26.

3 Y. F. Zhao, X. D. Jia, G. B. Chen, L. Shang, G. I. N. Waterhouse, L. Z. Wu, C. H. Tung, D. O'Hare and T. R. Zhang, Ultrafine NiO nanosheets stabilized by TiO$_2$ from monolayer NiTi-LDH precursors: an active water
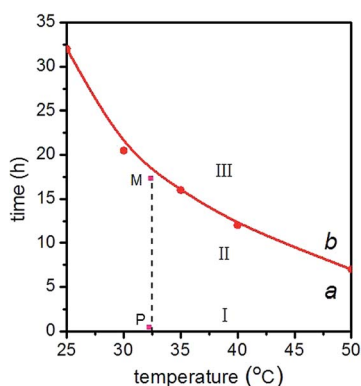
Fig. 11 The relationship between the temperature and time of the inflection points for the curves of $T-t$ and $\eta-t$. (I) Nanosheets cluster, (II) nanosheets cluster and dispersed nanosheets, and (III) stacked nanosheets.

oxidation electrocatalyst, *J. Am. Chem. Soc.*, 2016, **138**, 6517–6524.

4 Z. H. Li, M. F. Shao, H. L. An, Z. X. Wang, S. M. Xu, M. Wei, D. G. Evans and X. Duan, Fast electrosynthesis of Fe-containing layered double hydroxide arrays toward highly efficient electrocatalytic oxidation reactions, *Chem. Sci.*, 2015, **6**, 6624–6631.

5 C. Manzi-Nshuti, J. M. Hossenlopp and C. A. Wilkie, Comparative study on the flammability of polyethylene modified with commercial fire retardants and a zinc aluminum oleate layered double hydroxide, *Polym. Degrad. Stab.*, 2009, **94**, 782–788.

6 B. Nagendra, K. Mohan and E. B. Gowd, Polypropylene/layered double hydroxide (LDH) nanocomposites: influence of LDH particle size on the crystallization behavior of polypropylene, *ACS Appl. Mater. Interfaces*, 2015, **7**, 12399–12410.

7 L. Qiu, Y. S. Gao, X. R. Yan, J. Guo, A. Umar, Z. H. Guo and Q. Wang, Morphology-dependent performance of Mg_3Al–CO_3 layered double hydroxide as a nanofiller for polypropylene nanocomposites, *RSC Adv.*, 2015, **5**, 51900–51911.

8 X. J. Pang, X. M. Ma, D. X. Li and W. G. Hou, Synthesis and characterization of 10-hydroxycamptothecin-sebacate-layered double hydroxide nanocomposites, *Solid State Sci.*, 2013, **16**, 71–75.

9 C. H. Wang, X. Zhang, Z. T. Xu, X. Z. Sun and Y. W. Ma, Ethylene glycol intercalated Cobalt/Nickel layered double hydroxide nanosheet assemblies with ultrahigh specific capacitance: structural design and green synthesis for advanced electrochemical storage, *ACS Appl. Mater. Interfaces*, 2015, **7**, 19601–19610.

10 J. Plank, Z. Dai, H. Keller, F. v. Hössle and W. Seidl, Fundamental mechanism for polycarboxylate intercalation into C_3A hydrate phases and the role of sulfate present in cement, *Cem. Concr. Res.*, 2010, **40**, 45–57.

11 Z. P. Xu, G. S. Stevenson, C. Q. Lu, G. Q. Lu, P. F. Bartlett and P. P. Gray, Stable suspension of layered double hydroxide nanoparticles in aqueous solution, *J. Am. Chem. Soc.*, 2006, **128**, 36–37.

12 Y. Zhao, F. Li, R. Zhang, D. G. Evans and X. Duan, Preparation of layered double-hydroxide nanomaterials with a uniform crystallite size using a new method involving separate nucleation and aging steps, *Chem. Mater.*, 2002, **14**, 4286–4291.

13 S. Kannan, Influence of synthesis methodology and post treatments on structural and textural variations in $MgAlCO_3$ hydrotalcite, *J. Mater. Sci.*, 2004, **39**, 6591–6596.

14 M. Y. Ren, M. Yang, S. L. Li, G. W. Chen and Q. Yuan, High throughput preparation of magnesium hydroxide flame retardant *via* microreaction technology, *RSC Adv.*, 2016, **6**, 92670–92681.

15 S. Tao, M. Yang, H. H. Chen, M. Y. Ren and G. Chen, Continuous synthesis of hedgehog-like Ag–ZnO nanoparticles in a two-stage microfluidic system, *RSC Adv.*, 2016, **6**, 45503–45511.

16 H. H. Chen, M. Yang, S. Tao, M. Y. Ren and G. Chen, Facile synthesis of Co_3O_4 with different morphologies *via* oxidation kinetic control and its application in hydrogen peroxide decomposition, *Cryst. Growth Des.*, 2016, **16**, 6286–6293.

17 M. Y. Ren, M. Yang, G. W. Chen and Q. Yuan, High-throughput preparation of monodispersed layered double hydroxides *via* microreaction technology, *J. Flow Chem.*, 2014, **4**, 163–166.

18 Q. Wang and D. O'Hare, Recent advances in the synthesis and application of layered double hydroxide (LDH) nanosheets, *Chem. Rev.*, 2012, **112**, 4124–4155.

19 Z. An and J. He, Direct electronic communication at bio-interfaces assisted by layered-metal-hydroxide slab arrays with controlled nano-micro structures, *Chem. Commun.*, 2011, **47**, 11207–11209.

20 J. B. Han, J. Lu, M. Wei, Z. L. Wang and X. Duan, Heterogeneous ultrathin films fabricated by alternate assembly of exfoliated layered double hydroxides and polyanion, *Chem. Commun.*, 2008, 5188–5190.

21 W. Stephan, W. L. Vincent, H. Stephan, D. Viola, C. S. Hauke and V. L. Bettina, Cationically charged $Mn^{II}Al^{III}$ LDH nanosheets by chemical exfoliation and their use as building blocks in graphene oxide-based materials, *Langmuir*, 2013, **29**, 9199–9207.

22 G. Jia, Y. F. Hu, Q. F. Qian, Y. F. Yao, S. Y. Zhang, Z. S. Li and Z. G. Zou, Formation of hierarchical structure composed of (Co/Ni)Mn-LDH nanosheets on MWCNT backbones for efficient electrocatalytic water oxidation, *ACS Appl. Mater. Interfaces*, 2016, **8**, 14527–14534.

23 Y. F. Zhao, B. Li, Q. Wang, W. Gao, C. J. Wang, M. Wei, D. G. Evans, X. Duan and D. O'Hare, NiTi-layered double hydroxides nanosheets as efficient photocatalysts for oxygen evolution from water using visible light, *Chem. Sci.*, 2014, **5**, 951–958.

24 G. Hu and D. O'Hare, Unique layered double hydroxide morphologies using reverse microemulsion synthesis, *J. Am. Chem. Soc.*, 2005, **127**, 17808–17813.

25 D. J. Liang, W. B. Yue, G. B. Sun, D. Zheng, K. Ooi and X. J. Yang, Direct synthesis of unilamellar MgAl-LDH nanosheets and stacking in aqueous solution, *Langmuir*, 2015, **31**, 12464–12471.

26 X. J. Pang, M. Y. Sun, X. M. Ma and W. G. Hou, Synthesis of layered double hydroxide nanosheets by coprecipitation using a T-type microchannel reactor, *J. Solid State Chem.*, 2013, **210**, 111–115.

27 X. J. Pang, Y. Liu, L. Chen and Z. L. Quan, Fabrication and characterization of (hydroxyl camptothecin@sodium cholate)-layered double hydroxide nanohybrids, *Chem. Res. Chin. Univ.*, 2015, **36**, 1933–1938.

28 X. J. Pang, Y. Liu, L. Chen and Z. L. Quan, Fabrication of HCPT-LDH nanohybrids *via* co-assembly method and its characterization, *Chem. Res. Chin. Univ.*, 2016, **3**, 567–572.

29 X. J. Pang, J. J. Dai, Y. Liu, L. Chen, M. J. Chi, Y. T. Wang and Z. F. Li, Preparation of Zn–Al layered double hydroxide nanosheets by microchannel reactor and fabrication of LDH-based hydrophobic films, *Chem. Res. Appl.*, 2016, **28**, 1114–1119.

30 J. W. Boclair and P. S. Braterman, Relative stabilities of layered double hydroxides and simple counterparts, *Chem. Mater.*, 1999, **11**, 298–302.

31 J. W. Boclair, P. S. Braterman, J. Jiang, S. Lou and F. Yarberry, Formation of Cr(III) – containing layered double hydroxides directly from solution, *Chem. Mater.*, 1999, **11**, 303–307.

32 A. A. Eliseev, A. V. Lukashin, A. A. Vertegel, V. P. Tarasov and Y. D. Tret'yakov, A study of crystallization of Mg–Al double hydroxides, *Dokl. Chem.*, 2002, **387**, 339–343.

33 Z. Chang, C. Y. Wu, S. Song, Y. Kuang, X. D. Lei, L. R. Wang and X. M. Sun, Synthesis mechanism study of layered double hydroxides based on nanoseparation, *Inorg. Chem.*, 2013, **52**, 8694–8698.

34 J. Wang, J. Zhou, Z. Li, Y. Song, Q. Liu, Z. Jiang and M. Zhang, Magnetic, luminescent Eu-doped Mg–Al layered double hydroxide and its intercalation for ibuprofen, *Chem.–Eur. J.*, 2010, **16**, 14404–14411.

35 Z. Liu, R. Ma, Y. Ebina, N. Iyi, K. Takada and T. Sasaki, General synthesis and delamination of highly crystalline transition-metal-bearing layered double hydroxides, *Langmuir*, 2007, **23**, 861–867.

36 K. Okamoto, T. Sasaki, T. Fujita and N. Iyi, Preparation of highly oriented organic-LDH hybrid films by combining the decarbonation, anion-exchange and delamination processes, *J. Mater. Chem.*, 2006, **16**, 1608–1616.

37 V. N. Vikrant and V. Sukumaran, Sol–gel transition in dispersion of layered double hydroxide nanosheets, *Langmuir*, 2011, **27**, 13276–13283.

38 H. V. Olphen, Rheological phenomena of clay sols in connection with the charge distribution on the micelles, *Discuss. Faraday Soc.*, 1951, **11**, 82–84.

39 K. Norrish, The swelling of montmorillonite, *Discuss. Faraday Soc.*, 1954, **18**, 120–134.